VOLUME 71, NUMBER 24 PHYSICAL REVIEW LETTERS 13 DECEMBER 1993

Universal Subgap Optical Conductivity in Quasi-One-Dimensional Peierls Systems

Kihong Kim, Ross H. McKenzie, and John W. Wilkins
Department of Physics, The Ohio State University, Columbus, Ohio 43210

(Received 26 July 1993)

Quasi-one-dimensional Peierls systems with quantum and thermal lattice fluctuations can be modeled by a Dirac-type equation with a Gaussian-correlated off-diagonal disorder. A powerful new method gives the exact disorder-averaged Green function used to compute the optical conductivity. The strong subgap tail of the conductivity has a universal scaling form. The frequency and temperature dependence of the calculated spectrum agrees with experiments on KCP(Br) and *trans*-polyacetylene.

PACS numbers: 71.38.+i, 71.45.Lr

The interesting new physics exhibited by quasi-one-dimensional electronic materials continues to expand as advances in synthetic chemistry [1] and semiconductor fabrication technology [2] make new materials available for study. Many quasi-one-dimensional materials undergo a structural instability known as the Peierls or charge-density-wave instability [3–5]. Each chain has a periodic lattice distortion with twice the Fermi wave vector, $2k_F$, resulting in a gap 2Δ in the electronic spectrum at the Fermi surface, suggesting that such a gap should be clearly visible in the optical absorption spectrum. However, over the past twenty years, optical absorption measurements on a wide range of materials [6–8] have consistently shown that there is a broad tail below the gap. Moreover, as the temperature increases the spectrum broadens considerably. There is no accepted quantitative theory of the shape of the spectrum or its temperature dependence. While considerable effort has been made to understand excitation energies of solitons and polarons [3] in these compounds, there is also no accepted theory for their absorption spectrum.

The zero-point and thermal lattice motions have a significant effect on the electronic properties of the Peierls state and are, we believe, key to understanding the subgap absorption [9]. A recent luminescence and Raman study of a metal halogen mixed-valence (MX chain) compound produced results consistent with this view [10]. If the relevant phonon frequency at $q = 2k_F$, ω_{2k_F}, is much smaller than the optical frequency, as is the case in the optical absorption in most Peierls materials, the quantum and thermal lattice fluctuations can be modeled [9,11] by a static, Gaussian-random, backscattering potential, $\xi(x)$, with zero mean. Further, if the phonon dispersion near $q = 2k_F$ is ignored, $\xi(x)$ is fully characterized by the disorder-averaged correlator $\langle \xi(x)\xi^*(y)\rangle = \gamma\delta(x-y)$. In general, the dimensionless disorder parameter $\eta \equiv \gamma/\hbar v_F\Delta$, where v_F is the Fermi velocity, has contributions from extrinsic disorder such as due to impurities, η_e, as well as from the intrinsic disorder due to lattice fluctuations, η_i. The latter is related to the dimensionless electron-phonon coupling constant λ, the phonon frequency at $2k_F$, and temperature [9]:

$$\eta(T) = \eta_e + \eta_i(T) = \eta_e + \lambda\frac{\pi\hbar\omega_{2k_F}}{2\Delta}\coth\left(\frac{\hbar\omega_{2k_F}}{2k_BT}\right). \quad (1)$$

In this Letter, we develop a novel and powerful method for computing the electronic properties of one-dimensional Peierls semiconductors with static disorder. We use this method to calculate the real part of the optical conductivity. We find (1) a strong subgap tail in the optical absorption; (2) the remarkable fact that the *sub*gap conductivity, when properly scaled, follows a universal scaling curve independent of the disorder parameter η; (3) good agreement between the computed conductivity and the experimental conductivity for KCP(Br) [6] and *trans*-polyacetylene [7]; and (4) a universal scaling curve for the experimental conductivity for KCP(Br) at different temperatures with η having the temperature dependence given by Eq. (1). Figure 1 contrasts the relatively good agreement with experiment achieved by our calculation against that for a Lorentzian convolution of

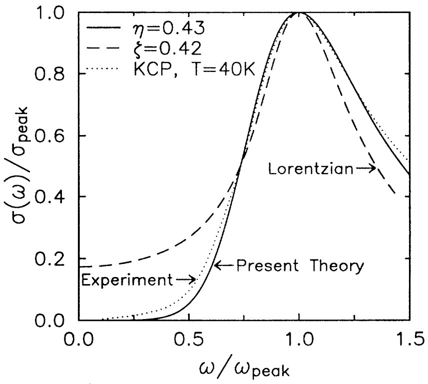

FIG. 1. Comparison of the real part of the frequency-dependent conductivity, $\sigma(\omega)$, obtained from our calculations for a disorder parameter $\eta = 0.43$ with experiment on KCP(Br) at $T = 40$ K [6] and the conductivity obtained from a Lorentzian convolution of the rigid-lattice conductivity for a dimensionless damping parameter $\zeta = 0.42$ [12]. The frequency and the conductivity are scaled by the frequency at the peak, ω_{peak}, and by $\sigma_{\text{peak}} = \sigma(\omega_{\text{peak}})$, respectively.

0031-9007/93/71(24)/4015(4)$06.00

the rigid-lattice conductivity [12].

We consider the standard continuum model [11,13] of noninteracting electrons in one dimension with a Peierls ground state, which, without the random term, has been studied extensively (see p. 795 in [3]) to understand the soliton and polaron excitations in conducting polymers. Our system is described by a Dirac-type equation [14] for the wave functions $\psi_1(x)$ and $\psi_2(x)$ for electrons moving with v_F to the right and to the left, respectively, in the interval $-L \leq x \leq L$ with a complex, Gaussian-random, backscattering potential $\xi(x)$:

$$\begin{pmatrix} -i\hbar v_F \dfrac{\partial}{\partial x} & \Delta + \xi(x) \\ \Delta + \xi^*(x) & i\hbar v_F \dfrac{\partial}{\partial x} \end{pmatrix} \begin{pmatrix} \psi_1(x) \\ \psi_2(x) \end{pmatrix} = E \begin{pmatrix} \psi_1(x) \\ \psi_2(x) \end{pmatrix}, \quad \langle \xi(x) \rangle = \langle \xi(x)\xi(y) \rangle = 0, \ \langle \xi(x)\xi^*(y) \rangle = \gamma\delta(x-y). \tag{2}$$

The above equations correspond to the case where the Fermi wavelength of the electron is incommensurate with the lattice period [15]. Previous work has succeeded in computing the density of states and localization length for this model [16]. Here we report the first exact calculation of the Green function [17].

We use G^+ (G^-), the retarded (advanced) 2×2 matrix Green function to compute the real part of the frequency-dependent conductivity for $\hbar\omega \gg k_B T$ [14,18]:

$$\sigma(\omega) = \frac{e^2}{A\hbar}\frac{2}{\pi\hbar\omega}\int_{-\hbar\omega}^{0} dE \int_{y}^{\infty} dx \ \mathrm{Re}\left[j^{+-}(E+\hbar\omega, E|x-y) - j^{++}(E+\hbar\omega, E|x-y) \right], \tag{3}$$

where A is the cross-sectional area of a chain and

$$j^{\pm\pm}(E', E|x-y) = (\hbar v_F)^2 \langle \mathrm{Tr}\left[\sigma_3 G^{\pm}(y,x|E')\sigma_3 G^{\pm}(x,y|E) \right] \rangle. \tag{4}$$

σ_3 is a Pauli matrix. Here we report the computation of the conductivity using the approximation $\langle GG \rangle \approx \langle G \rangle \langle G \rangle$, which we expect to be valid for $\hbar\omega \gg \gamma/\hbar v_F$, i.e., for optical but not dc conductivities. However, our method can be used to compute $\langle GG \rangle$ directly.

Exact calculation of the Green function.—Two linearly independent wave functions ψ and $\tilde{\psi}$ satisfy the boundary conditions $\psi(-L) = 1$ and $\tilde{\psi}(L) = 1$. These ψ and $\tilde{\psi}$ will be statistically independent in the limit $L \to \infty$ [14]. For $x > y$,

$$G(x,y|E) = \frac{i}{\hbar v_F(\psi_1\tilde{\psi}_2 - \psi_2\tilde{\psi}_1)} \begin{pmatrix} \tilde{\psi}_1(x)\psi_2(y) & \tilde{\psi}_1(x)\psi_1(y) \\ \tilde{\psi}_2(x)\psi_2(y) & \tilde{\psi}_2(x)\psi_1(y) \end{pmatrix}, \tag{5}$$

where $(\psi_1\tilde{\psi}_2 - \psi_2\tilde{\psi}_1)$ is a constant independent of x. We obtain G^+ (G^-) by solving for wave functions with ImE a small positive (negative) number. Then the denominator can be Taylor expanded and

$$G^+(x,y|E) = -\frac{i}{\hbar v_F}\sum_{n=0}^{\infty} \begin{pmatrix} \hat{C}_n(x,y)\hat{y}_n(x) & \hat{D}_n(x,y)\hat{y}_n(x) \\ \hat{C}_n(x,y)\hat{y}_{n+1}(x) & \hat{D}_n(x,y)\hat{y}_{n+1}(x) \end{pmatrix}, \tag{6}$$

where

$$\hat{y}_n(x) = \left[\frac{\tilde{\psi}_2(x)}{\tilde{\psi}_1(x)}\right]^n, \quad \hat{C}_n(x,y) = \left[\frac{\psi_1(x)}{\psi_2(x)}\right]^n \frac{\psi_2(y)}{\psi_2(x)}, \quad \hat{D}_n(x,y) = \left[\frac{\psi_1(x)}{\psi_2(x)}\right]^n \frac{\psi_1(y)}{\psi_2(x)}. \tag{7}$$

Next, we take the $L \to \infty$ limit and utilize the statistical independence of ψ and $\tilde{\psi}$ to factor the average of the Green function into products of averages of $\hat{C}$ ($\hat{D}$) and $\hat{y}$. The quantities $C_n \equiv \langle \hat{C}_n(x,y) \rangle$ and $D_n \equiv \langle \hat{D}_n(x,y) \rangle$ are functions of $(x-y)$ and $y_n \equiv \langle \hat{y}_n(x) \rangle$ is independent of x. Thus the averaged Eq. (6) can be written in terms of y_n, $C_n(x-y)$, and $D_n(x-y)$. The following equations for y_n and C_n can be derived from Eq. (2) using standard Fokker-Planck methods [19], subject to the conditions $y_0 = 1$ and $C_n(0) = y_n$, which follow from Eq. (7) for y_0, and from Eq. (7) and the equality $\langle (\tilde{\psi}_2/\tilde{\psi}_1)^n \rangle = \langle (\psi_1/\psi_2)^n \rangle$ [14] for $C_n(0)$:

$$\left(2\frac{E}{\Delta} + i\eta n\right) y_n - y_{n+1} - y_{n-1} = 0, \tag{8}$$

$$\frac{\hbar v_F}{\Delta}\frac{dC_n}{d(x-y)} = i(2n+1)\frac{E}{\Delta}C_n - i(n+1)C_{n+1} - inC_{n-1} - \eta\left(n^2 + n + \tfrac{1}{2}\right)C_n. \tag{9}$$

D_n satisfies the same equation as C_n with the initial condition $D_n(0) = y_{n+1}$.

The key to our method is the fact that y_n, C_n, and D_n decay very rapidly and exponentially as a function of n.—The decay rate is determined by the dimensionless disorder parameter $\eta = \gamma/\hbar v_F\Delta$: the larger η, the more rapid the decay. To solve Eqs. (8) and (9) numerically, we truncate the number of equations by setting $y_n = 0$ for $n > N$. For example, at $\eta = 0.1$, the Green function

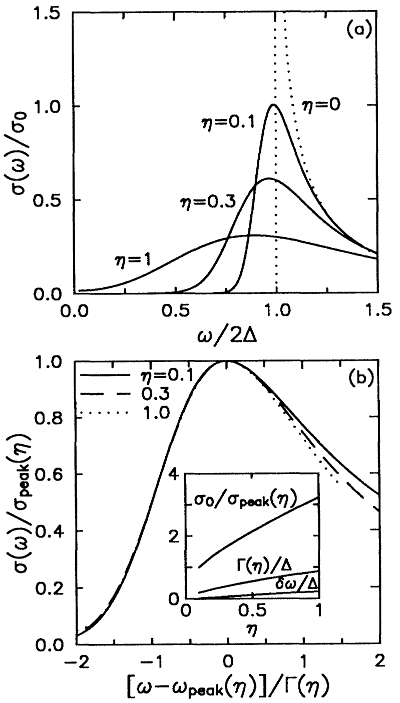

FIG. 2. Universal form of the computed subgap optical conductivity. (a) Conductivity spectrum for different values of the disorder parameter η [Eq. (1)]. The spectrum broadens as η increases. The conductivity scale is set by $\sigma_0 = e^2 v_F / A\Delta$, where A is the cross-sectional area of a chain. (b) Scaling plot of $\sigma(\omega)$, where the frequency is scaled by $\Gamma(\eta)$, the half-width for the low frequency side of the peak. Note we claim only that the *sub*gap ($\omega < \omega_{\text{peak}}$) conductivity scales. Inset: Dependence on the disorder parameter η of σ_{peak}, Γ, and $\delta\omega(\eta) \equiv 2\Delta - \omega_{\text{peak}}(\eta)$.

is converged to 1 ppm for $N = 30$. The method can be generalized to the calculation of $\langle GG \rangle$. The number of resulting equations scales as N^2.

We calculate the conductivity using the exact Green function obtained by solving Eqs. (8) and (9) and the approximation $\langle GG \rangle \approx \langle G \rangle \langle G \rangle$. In Fig. 2(a) we show the result for several different η values. The $\eta = 0$ curve shows no absorption below the energy gap and a divergent behavior just above the gap. For finite η values, the singularity is absent, and the spectrum broadens rapidly as η increases. In the inset of Fig. 2(b) we plot the dependence on η of three quantities characterizing the shape of the conductivity curve: Γ, which is the half-width for the low frequency side of the peak, the inverse of the conductivity at the peak, and $\delta\omega$, the shift of the peak frequency from 2Δ. Quite remarkably, when we scale the conductivity by the peak value and the frequency by Γ, we find that the scaled curves for all η values have *a universal form independent of* η below the peak frequency [20,21].

Experimental data on the platinum, linear-chain compound $K_2Pt(CN)_4Br_{0.3}{\cdot}3H_2O$ or KCP(Br) [6] show a similar scaling behavior. In Fig. 3 we plot the data for five temperatures. The scaling curve below the conductivity peak has approximately the same form as the theoretical curve in Fig. 2(b). We deduce the effective disorder parameter for each temperature by choosing η such that the computed $\Gamma(\eta)/\omega_{\text{peak}}(\eta)$ [22] is equal to $\Gamma(T)/\omega_{\text{peak}}(T)$. This criterion was used to choose the value $\eta = 0.43$ in Fig. 1. In the inset of Fig. 3 we plot the η values thus determined versus temperature. The temperature dependence of η is compared with the postulated form (1): an extrinsic temperature-independent η_e plus an intrinsic temperature-dependent η_i. The fit value of extrinsic disorder is large. This is not surprising since x-ray and neutron scattering studies have shown that the bromine ions randomly occupy two different sites [23]. This disorder could cause significant scattering of the electrons along the platinum chains [24].

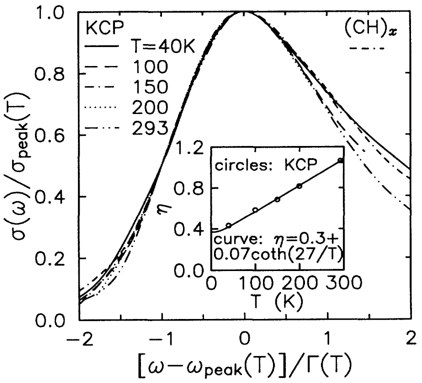

FIG. 3. Scaling plot of experimental data for KCP(Br) [6] and *trans*-$(CH)_x$ [7] at different temperatures. For each temperature, the corresponding disorder parameter value is obtained by choosing η such that the theoretical $\Gamma(\eta)/\omega_{\text{peak}}(\eta)$ value is equal to $\Gamma(T)/\omega_{\text{peak}}(T)$. Inset: Comparison of the temperature dependence of η for KCP(Br) with Eq. (1). We fit the data with a curve in which the first number (0.3) characterizes extrinsic disorder effects and the second number [$\eta_i(0) = 0.07$] depends sensitively on the value of ω_{2k_F} (twice the third number in K) which we took from experiment [5]. The possibility of the scaling curve extending to temperatures above the three-dimensional ordering transition at $T_P = 120$ K [5] is based on the persistence of a "pseudogap" above T_P [25].

We have analyzed the optical conductivity data for *trans*-polyacetylene $(CH)_x$ at room temperature [7]. Since the phonon frequency at $2k_F$ for this material is at a much larger energy scale than the room temperature, the optical conductivity does not depend sensitively on temperature. Consequently, unlike in KCP(Br), we cannot determine the separate contributions from extrinsic and intrinsic disorder. In Fig. 3, we show that the scaled $(CH)_x$ *sub*gap conductivity curve agrees well with those of KCP(Br).

The peak of the conductivity is the product of $\sigma_0 \equiv e^2 v_F / A\Delta$ and the dimensionless ratio $\sigma_{\text{peak}}(\eta)/\sigma_0$ determined from fitting the experimental curves. Accordingly the peak conductivity yields σ_0 and hence v_F since the

TABLE I. Fermi velocity v_F and disorder parameter η determined from fits of experimental optical conductivity to our calculations. The peak height determines v_F which is compared to the results of band structure calculations [3,5]. The η values obtained from the fits are compared to the intrinsic $\eta_i(T=0) = (\delta u/u_0)^2(\Delta a/\hbar v_F)$, calculated using the band structure v_F, and the zero-point motion δu and lattice distortion u_0 in Table I of Ref. [9]. The electron-phonon coupling λ is calculated from the estimated value of η_i and Eq. (1).

	v_F (10^7cm/sec)		η		
	Fit	Band structure	Fit	Estimate of η_i	λ
KCP(Br)	5.2	11.0	η_e=0.3, $\eta_i(0)$=0.07	0.07	0.96
$(CH)_x$	7.1	9.3	$\eta_e+\eta_i(0)$=0.15	0.18	0.48

gap 2Δ and cross-sectional area A are known. Table I shows that the v_F's obtained this way are smaller than estimates based on band structure calculations. The values of $\eta_i(T=0)$ for KCP(Br) and $\eta(T=0)$ for $(CH)_x$ obtained from the fitting are compared with estimates from the lattice zero-point motion.

In conclusion, we have developed a new method for computing the electronic properties of quasi-one-dimensional Peierls systems including disorder and lattice fluctuation effects and used it to obtain the absorptive conductivity at all temperatures. Our results compare well with data on KCP(Br) and *trans*-polyacetylene. The *sub*gap conductivity curve has a universal scaling form.

We thank Leo Degiorgi for helpful discussions and for showing us his results before publication. This research has been supported in part by the U.S. DOE, Basic Energy Sciences, Division of Materials Sciences, and the OSU Center for Materials Research.

---

[1] *Proceedings of the International Conference on Science and Technology of Synthetic Metals, Göteberg, Sweden, 12–18 August 1992* [Synth. Met. **55–57** (1993)].

[2] For a discussion of quantum wires see, e.g., C. Weisbuch and B. Vinter, *Quantum Semiconductor Structures* (Academic, Boston, 1991), Chap. 6.

[3] A. J. Heeger, S. Kivelson, J. R. Schrieffer, and W.-P. Su, Rev. Mod. Phys. **60**, 781 (1988). For $(CH)_x$, $v_F = 2t_0a/\hbar$ where $4t_0 = 10$ eV is the tight-binding bandwidth and $a = 1.24$ Å is the intrachain atomic separation. The cross-sectional area per chain $A = 1.55 \times 10^{-15}$ cm^2.

[4] G. Grüner, Rev. Mod. Phys. **60**, 1129 (1988).

[5] K. Carneiro, in *Electronic Properties of Inorganic Quasi-One-Dimensional Compounds, Part II*, edited by P. Monceau (Reidel, Dordrecht, 1985), p. 1. KCP(Br) has a free-electron-like band, $v_F = \hbar k_F/m$. $k_F = 0.94$ Å^{-1}. $A = 4.90 \times 10^{-15}$ cm^2.

[6] P. Brüesch, S. Strässler, and H. R. Zeller, Phys. Rev. B **12**, 219 (1975) [KCP(Br)]. KCP(Br) is an acronym for $K_2Pt(CN)_4Br_{0.3} \cdot 3(H_2O)$.

[7] G. Leising, Phys. Rev. B **38**, 10313 (1988) [$(CH)_x$].

[8] R. P. McCall *et al.*, Phys. Rev. B **39**, 7760 (1989) (TCNQ compounds); D. Berner *et al.*, J. Phys. (France) IV C2 **3**, 255 (1993) [$(TaSe_4)_2I$]; L. Degiorgi, J. Phys. IV (France), Colloq. **3**, C2-103 (1993) ($K_{0.3}MoO_3$).

[9] R. H. McKenzie and J. W. Wilkins, Phys. Rev. Lett. **69**, 1085 (1992); Synth. Met. **55–57**, 4296 (1993).

[10] F. H. Long, S. P. Love, B. I. Swanson, and R. H. McKenzie, Phys. Rev. Lett. **71**, 762 (1993).

[11] S. A. Brazovskii and I. E. Dzyaloshinskii, Zh. Eksp. Teor. Fiz. **71**, 2338 (1976) [Sov. Phys. JETP **44**, 1233 (1976)].

[12] If we convolute the rigid-lattice conductivity with a Lorentzian, we obtain

$$\sigma(\omega) = \frac{2}{\pi}\frac{\Delta}{\omega}\mathrm{Im}\int_0^\infty dx\,\frac{1}{\sqrt{1+x^2}[1+x^2-(\omega/\Delta+i\zeta)^2/4]},$$

where $\zeta\Delta$ corresponds to an energy-independent damping of the transition. Z.-b. Su and L. Yu [Commun. Theor. Phys. (Beijing) **2**, 1341 (1983)] previously pointed out that this form does not agree quantitatively with the observed subgap absorption.

[13] H. Takayama, Y. R. Lin-Liu, and K. Maki, Phys. Rev. B **21**, 2388 (1980).

[14] A. A. Ovchinnikov and N. S. Érikhman, Zh. Eksp. Teor. Fiz. **78**, 1448 (1980) [Sov. Phys. JETP **51**, 728 (1980)].

[15] In particular, the condition $\langle\xi(x)\xi(y)\rangle = 0$ implies that there is no umklapp scattering. A nonzero value occurs for a *real* random backscattering potential which corresponds to the half-filled band (commensurate) case, an example of which is polyacetylene $(CH)_x$.

[16] H. J. Fischbeck and R. Hayn, Phys. Status Solidi (b) **158**, 565 (1990), and references therein.

[17] Our method can be further generalized to the case with forward, backward, and umklapp scattering processes. In fact, we can reproduce the results of previous density of states calculations [16] with great efficiency.

[18] J. Rammer and H. Smith, Rev. Mod. Phys. **58**, 323 (1986).

[19] I. M. Lifshits, S. A. Gredeskul, and L. A. Pastur, *Introduction to the Theory of Disordered Systems* (Wiley, New York, 1988), p. 146.

[20] This universal behavior is quite distinct from that obeyed by the Urbach tails seen in three-dimensional crystalline and amorphous semiconductors.

[21] The scaling curve in Fig. 2(b) below the absorption peak is fitted with the function $\sigma(\omega)/\sigma(\omega_{\text{peak}}) = \exp[-0.49|(\omega-\omega_{\text{peak}})/\Gamma|^2 - 0.20|(\omega-\omega_{\text{peak}})/\Gamma|^3]$.

[22] The dependence of $\Gamma/\omega_{\text{peak}}$ on the disorder parameter η can be fitted by $\Gamma(\eta)/\omega_{\text{peak}}(\eta) = \eta^{0.62}(0.414 + 0.077\eta)$.

[23] J. M. Williams *et al.*, Phys. Rev. Lett. **33**, 1079 (1974).

[24] H. Wagner *et al.*, Solid State Commun. **13**, 659 (1973).

[25] P. A. Lee, T. M. Rice, and P. W. Anderson, Phys. Rev. Lett. **31**, 462 (1973); M. J. Rice and S. Strässler, Solid State Commun. **13**, 1389 (1973).